Journal of Applied Fluid Mechanics, Vol. 9, No. 2, pp. 925-934, 2016.
Available online at www.jafmonline.net, ISSN 1735-3572, EISSN 1735-3645.
DOI: 10.18869/acadpub.jafm.68.225.24163

Three-Dimensional Unsteady Stagnation-Point Flow and Heat Transfer Impinging Obliquely on a Flat Plate with Transpiration

M. H. Haddad Sabzevar, A. B. Rahimi† and H. Mozayeni

Faculty of Engineering, Ferdowsi University of Mashhad, P.O. Box No. 91775-1111, Mashhad, Iran

†*Corresponding Author Email: rahimiab@yahoo.com*

(Received October 16, 2014; accepted February 25, 2015)

ABSTRACT

In this study, an exact solution of the Navier-Stokes and energy equations is obtained for the problem of unsteady three-dimensional stagnation point flow and heat transfer of viscous, incompressible fluid on a flat plate. An external flow with strain rate $a/(1-at)$ impinges obliquely on the flat plate when the plate is assumed to be with transpiration. This flow consists of an irrotational stagnation-point flow (Hiemenz) and a tangential component. The relative importance of these two flows is measured by a parameter γ. Appropriate similarity transformations are introduced, for the first time, to reduce the governing Navier-Stokes and energy equations to a coupled system of ordinary differential equations. The fourth-order Runge-Kutta method along with a shooting technique is applied to numerically solve the ordinary differential equations. The results obtained from numerical procedure are presented and discussed for a wide range of parameters characterizing the problem. The results achieved reveal that the transpiration rate has a considerable effect on the distributions of velocity components, temperature and pressure. Moreover, it is shown that the main consequence of the free stream obliqueness is to move the stagnation point away from the origin of the coordinate system.

Keywords: Exact solution; Similarity transformations; Obliqueness; Transpiration.

NOMENCLATURE

a	flow strain rate	$\bar{x},\bar{y},\bar{z}$	dimensionless Cartesian coordinates
b	constant		
f,g,h	similarity functions	α	thermal diffusion
Pr	Prandtl number	η	similarity variable
p	pressure	μ	dynamic viscosity
S	dimensionless transpiration rate	θ	dimensionless temperature
T	temperature	γ	ratio of shear flow to normally impinging flow
t	time		
$\bar{t}$	dimensionless time	λ	velocity ratio
u,v,w	velocity components near the plate in x, y and z directions	ρ	density
		υ	kinematic viscosity
$\bar{u},\bar{v},\bar{w}$	dimensionless velocity components near the plate in x, y and z directions	τ	surface shear stress
		τ_x,τ_y	shear stress components in x and directions
U,V,W	potential region velocity components in x, y and z directions	0	stagnation point
		w	wall
W_0	transpiration rate	∞	infinite

1. INTRODUCTION

The study of stagnation flow and heat transfer of a

viscous fluid in the vicinity of a plate or cylinder has been of considerable interest during the last decades. It is because of its great technical importance in many branches of industrial applications such as drying of papers and films and high-pressure washers. Nonlinearity of the Navier-Stokes and energy equations has been always a technical problem for these equations to be solved. Hence, researches seek similarity methods to resolve this problem. By applying the similarity solution method, the Navier-Stokes and energy equations are reduced to ordinary differential equations which are much easier to numerically solve. There are some fundamental publications regarding the problem of stagnation flow in the vicinity of a body in the last years.

The two-dimensional and axisymmetric three-dimensional stagnation-point flows on a cylinder were firstly studied by Hiemenz (1911) and Homann (1936). Problem of stagnation flow against an axisymmetric flat plate was investigated by Howarth (1954) and Davey (1951). Afterwards, Chiam (1994), Mahapatra and Gupta (2002), Reza and Gupta (2005) along with Lok and Amin (2006) scrutinized the steady two-dimensional stagnation point flow of an incompressible viscous fluid over a flat deformable sheet. The sheet is stretched in its own plane with a velocity proportional to the distance from the stagnation point. The flow impinges on the wall either orthogonal or at an arbitrary angle of incidence. Also, Stuart (1959), Tamada (1979), Niimi et al. (1981) and Dorrepaal et al. (1986) obtained an exact solution of the Navier-Stokes equations representing the problem of two-dimensional stagnation-point flow of an incompressible viscous fluid impinging obliquely on a plane rigid wall. Afterwards, in Laboropulu et al. (1996), the obliquely impinging flow on a wall with suction or blowing was solved. Some other papers studied the steady or unsteady three-dimensional case of stagnation flow along with heat transfer on a flat plate. Firstly, unsteady three dimensional stagnation point flow was discussed by Cheng et al. (1971). In another research, Wang (1984) solved the three dimensional flow over a stretching flat surface. Devi et al. (1986) studied unsteady three dimensional boundary layer flows due to a stretching surface. Shokrgozar and Rahimi (2009) considered the three dimensional stagnation flow and heat transfer on a flat plat with transpiration. Besides, the problem of three dimensional boundary layer flows due to a permeable shrinking sheet was studied by Bachok (2010). The study of stagnation flow on a cylinder has been an interest of many researches so far. Gorla (1976, 1977, 1977, and 1978) in a series of papers studied the steady and unsteady stagnation flow and heat transfer in the vicinity of a circular cylinder for the cases of constant or axial movement. Furthermore, Axisymmetric and nonaxisymmetric stagnation-point flow and heat transfer of a viscous, incompressible fluid on a moving cylinder in different physical phenomena is the main subject of papers conducted by Saleh and Rahimi (2004) and Rahimi and Saleh (2007, 2008). They investigated the effects of different forms of axial and angular cylinder motion on velocity and temperature profiles. Stagnation point flow impinging obliquely on a cylinder has been; also, investigated by a number of authors. Firstly, Weidman (1976) conducted an investigation for the case of axisymmetric stagnation flow impinging obliquely on circular cylinder. After that, Rahimi and Esmaeilpour (2010) solved the problem of axisymmetric stagnation flow obliquely impinging on a moving circular cylinder with uniform transpiration. Also, Rahimi and Mossavinik (2007) studied axisymmetric stagnation point flow and heat transfer obliquely impinging on a rotating circular cylinder.

In this study, the exact solution of Navier-Stokes and energy equations is intended to be obtained for the problem of unsteady three dimensional stagnation point flow and heat transfer of a viscous, incompressible fluid impinging obliquely on a flat plate. The problem is investigated in the vicinity of the plate in the presence of suction and blowing effects. An external flow impinges obliquely on the flat plate with strain rate $a/(1-at)$. This flow consists of irrotational stagnation point flow (Hiemenz) and a tangential component. The governing equations are reduced to a coupled system of ordinary differential equations by using appropriate similarity transformations introduced for the first time. These ordinary equations are solved using numerical techniques. Velocity profiles, surface stress tensors, pressure profiles and temperature profiles are presented for a wide range of characterizing parameters.

2. PROBLEM FORMULATION

The problem of unsteady three-dimensional stagnation-point flow and heat transfer of a viscous, incompressible fluid impinging obliquely on a flat plate is aimed to solve for the first time. In order to solve this problem, three-dimensional Cartesian coordinate system (x, y, z) with corresponding velocity components (u, v, w) is selected, as it is illustrated in Fig. 1. An external potential flow impinges on the plate with strain rate $a/(1-at)$. This flow consists of irrotational stagnation point and a uniform shear flow parallel to the surface. The relative importance of these two flows is measured by the parameter γ. After impingement of the fluid on x-y plane, two separated regions are produced. These regions are the potential region and the region of rapid changes of velocity components in x and y directions. If the flow pattern on the plate is bounded from both sides in one of the directions, for example x-axis, because of some physical limitations, a difference between the values of x and y velocity components will be captured in the region of rapid changes. A parameter characterizing this situation is λ, the coefficient indicating the ratio of x to y velocity components in potential region when the flow impinges on the plate normally. This parameter is defined between 0 and 1, $0 < \lambda \leq 1$, Ref [3]. The flow will be the axisymmetric if $\lambda = 1$ and will be

considered the two-dimensional if $\lambda = 0$. In such a situation, there is no velocity component in x-direction. With the increase of λ from 0 to 1, the problem crosses the line from two-dimensionality to axisymmetric three-dimensionality.

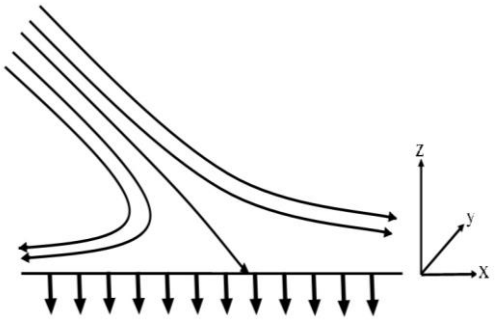

Fig. 1. Schematic of the problem.

The Navier-Stokes and enefffrgy equations governing this problem are as follow.

$$\frac{\partial u}{\partial x}+\frac{\partial v}{\partial y}+\frac{\partial w}{\partial z}=0 \tag{1}$$

$$\frac{\partial u}{\partial t}+u\frac{\partial u}{\partial x}+v\frac{\partial u}{\partial y}+w\frac{\partial u}{\partial z}=-\frac{1}{\rho}\frac{\partial p}{\partial x} +\upsilon\left[\frac{\partial^2 u}{\partial x^2}+\frac{\partial^2 u}{\partial y^2}+\frac{\partial^2 u}{\partial z^2}\right] \tag{2}$$

$$\frac{\partial v}{\partial t}+u\frac{\partial v}{\partial x}+v\frac{\partial v}{\partial y}+w\frac{\partial v}{\partial z}=-\frac{1}{\rho}\frac{p}{\partial x} +\upsilon\left[\frac{\partial^2 v}{\partial x^2}+\frac{\partial^2 v}{\partial y^2}+\frac{\partial^2 v}{\partial z^2}\right] \tag{3}$$

$$\frac{\partial w}{\partial t}+u\frac{\partial w}{\partial x}+v\frac{\partial w}{\partial y}+w\frac{\partial w}{\partial z}=-\frac{1}{\rho}\frac{\partial p}{\partial x} +\upsilon\left[\frac{\partial^2 w}{\partial x^2}+\frac{\partial^2 w}{\partial y^2}+\frac{\partial^2 w}{\partial z^2}\right] \tag{4}$$

$$\frac{\partial T}{\partial t}+u\frac{\partial T}{\partial x}+v\frac{\partial T}{\partial y}+w\frac{\partial T}{\partial z}= \alpha\left[\frac{\partial^2 T}{\partial x^2}+\frac{\partial^2 T}{\partial y^2}+\frac{\partial^2 T}{\partial z^2}\right] \tag{5}$$

Where $p, \rho, \upsilon, \alpha$ and T are the fluid pressure, density, kinematic viscosity, thermal diffusivity and temperature, respectively. It is worth noting that the dissipation terms of the energy equation are negligible at the stagnation region.

3. SELF-SIMILAR SOLUTIONS

3.1. Fluid Flow Solution

The velocity components and pressure term gained by solving the governing equations (1-4) in the potential region are expressed as follow, [9], [10] and [12],

$$U=\frac{a\lambda x}{1-at}+\frac{b z}{1-at} \tag{6}$$

$$V=\frac{a y}{1-at} \tag{7}$$

$$W=\frac{-a(1+\lambda)z-W_0}{1-at} \tag{8}$$

$$P_\infty = P_0-\frac{\rho}{(1-at)^2}\left[\frac{a^2\lambda(1+\lambda)}{2}(x^2+z^2) +a^2y^2-W_0(bx-a\lambda z)\right] \qquad ,0<\lambda\le 1 \tag{9}$$

Where a, p_0 and W_0 are a constant used in the strain rate relation, the stagnation pressure and the transpiration rate in z direction. Besides, b is a constant indicating the importance of shear flow to irrotational stagnation flow. Moreover, λ is a coefficient being the aspect ratio of potential velocity components in x to y directions when the flow impinges on the plate along z-direction. This parameter is defined between 0 and 1, as it was explained in section 2. The solution of the governing Navier-Stokes and energy equations (1-5) in the viscous region close to the plate must approach the solution of the outer inviscid flow. A reduction of the governing equations to ordinary differential equations in viscous region is accomplished by using suitably introduced new similarity transformations as bellow,

$$\eta=\frac{z}{\sqrt{1-at}}\sqrt{a/\upsilon} \tag{10}$$

$$u=\frac{ax\,\lambda f'(\eta)}{1-at}+\sqrt{\upsilon/a}\,\frac{b\,h(\eta)}{\sqrt{1-at}} \tag{11}$$

$$v=\frac{a y[f'(\eta)+g'(\eta)]}{1-at} \tag{12}$$

$$w=\frac{-\sqrt{a\upsilon}}{\sqrt{1-at}}\left((1+\lambda)f(\eta)+g(\eta)+\frac{W_0}{\sqrt{a\upsilon}}\right) \tag{13}$$

In the above relations, η is the similarity variable, the terms $f(\eta), g(\eta)$ and $h(\eta)$ are similarity function which appear in similarity solution and the prime denotes differentiation with respect to η. Moreover, t is the time which must be in the range of $-\infty < t \le \frac{1}{a}$, mathematically. It is worth noting that for the case of normally impinging flow $b \to 0$ with constant strain rate a, the similarity transformations introduced in (10) to (13) become similar to those obtained in Shokrgozar and Rahimi (2009).

Inserting the similarity transformations (10) to (13) into the governing equations (1) to (4) causes the Continuity equation to be satisfied, automatically, and gives a coupled system of ordinary differential equations reduced from x-momentum and y-

momentum and, also, an expression for the pressure, obtained by integrating Eq. (4) in z-direction, as follow,

$$f''' - \frac{1}{2}\eta f'' + \left((1+\lambda)f + g + S\right)f'' - \lambda f'^2 - f' + 1 + \lambda = 0 \quad (14)$$

$$g''' - \frac{1}{2}\eta g'' + \left((1+\lambda)f + g + S\right)g'' - g' - (2f' + g')g' - (1-\lambda)f'^2 - \lambda + 1 = 0 \quad (15)$$

$$h'' - \frac{1}{2}\eta h' + \left((1+\lambda)f + g + S\right)h' - \lambda h f' - \frac{1}{2}h - S = 0 \quad (16)$$

$$p = p_0 - \frac{\rho}{(1-at)^2}\left[\frac{a^2\lambda(1+\lambda)}{2}x^2 + a^2 y^2 - W_0 b x + \nu(1-at)\Phi(\eta)\right] \quad (17)$$

In which,

$$\Phi(\eta) = \frac{(1+\lambda)}{2}f\,\eta + \frac{1}{2}g\,\eta + \frac{1}{2}s\,\eta + \frac{(1+\lambda)^2}{2}f^2 + \frac{g^2}{2} + (1+\lambda)f\,g + (1+\lambda) + s\,g + (1+\lambda)f' + g' \quad (18)$$

In the above equations, S is the dimensionless transpiration rate and is defined as,

$$S = \frac{W_0}{\sqrt{a\nu}} \quad (19)$$

Note that $S > 0$ corresponds to suction into the plate and $S < 0$ refers to blowing out of it.

The needed boundary conditions for solving the set of similarity equations (14) to (16) are,

$$\eta = 0 : f = 0,\ f' = 0,\ g = 0,\ g' = 0,\ h = 0 \quad (20)$$

$$\eta \to \infty : f' = 1,\ h' = 1,\ g' = 0 \quad (21)$$

3.2. Heat Transfer Solution

To transform the energy equation into a dimensionless, similarity form for the case of defined wall temperature, we introduce

$$\theta = \frac{T(\eta) - T_\infty}{T_w - T_\infty} \quad (22)$$

In which, T_∞ is the free stream temperature and T_w is the wall temperature. Making use of similarity transformations (10) to (13) and (22), the energy equation is written as

$$\theta'' + \Pr\left((1+\lambda)f + g + S - \frac{1}{2}\eta\right)\theta' = 0 \quad (23)$$

Where Pr is the Prandtl number and is defined as,

$$\Pr = \frac{\nu}{\alpha} \quad (24)$$

The boundary conditions needed to solve the equation (23) are as follow,

$$\eta = 0 :\ \theta = 1 \quad (25)$$

$$\eta \to \infty :\ \theta = 0 \quad (26)$$

Besides, the heat loss per area from the plate can be obtained by using the following relation,

$$Q = k\frac{dT}{d\eta} = k\frac{1}{(1-\bar{t})^{1/2}}\left(\frac{a}{\upsilon}\right)^{1/2}(T_w - T_\infty)\,\theta'(0) \quad (27)$$

A finite difference procedure including tri-diagonal matrix algorithm (TDMA) is used to discretize the governing equations (14) to (18) and (23) describing the sets of laws. Also, the fourth-order Runge-Kutta method of integration along with a shooting method is applied to numerically solve the governing equations. The numerical procedure is repeated until the difference between the results of two repeated sequences of each of the equations becomes less than 0.00001.

The results are presented for different values of γ, λ, S and Pr numbers in section 4.

3.3. Shear Stress

The shear stress on z=0 plane is achieved by using the following relation,

$$\tau = \tau_x \vec{e}_x + \tau_y \vec{e}_y = \mu\left(\frac{\partial u}{\partial z}\vec{e}_x + \frac{\partial v}{\partial z}\vec{e}_y\right)_{z=0} \quad (28)$$

By using the similarity transformations introduced in relations (10) to (12), the shear stress components at the wall become,

$$\tau_x = \mu\frac{\partial u}{\partial z} = \mu\left(\frac{\lambda\bar{x}f''}{(1-\bar{t})^{3/2}} + \frac{\gamma h'}{1-\bar{t}}\right)_{z=0} \quad (29)$$

$$\tau_y = \mu\frac{\partial v}{\partial z} = \mu\left(\frac{\bar{y}(f'' + g'')}{(1-\bar{t})^{3/2}}\right)_{z=0} \quad (30)$$

There are some dimensionless parameters used in (29) and (30) equations. These parameters are defined as follow,

$$\gamma = \frac{b}{a\lambda},\quad \bar{x} = x\sqrt{\frac{a}{\nu}},\quad \bar{y} = y\sqrt{\frac{a}{\nu}},\quad \bar{t} = at \quad (31)$$

In which, $\bar{x}, \bar{y}$ and $\bar{t}$ are dimensionless forms of coordinates x, y and time. Moreover, μ is the dynamic viscosity. Besides, γ is the parameter indicating the relative importance between the normally impinging flow and the uniform shear flow parallel to the surface. If $\gamma \to 0$, the shear flow is negligible and in the case of $\gamma \to \infty$, the flow includes only shear flow.

In an obliquely impinging flow, the obliqueness causes the stagnation point to be shifted toward the

incoming flow in x-direction. In order to calculate the position of the stagnation point in an obliquely stagnation flow, equation (32) is introduced. In this equation, $\bar{x}_s$ is the distance between the origin of the coordinate system and the location of the stagnation point.

$$\bar{x}_s = -\frac{\gamma h'(0)}{f''(0)}(1-\bar{t})^{1/2} \tag{32}$$

4. PRESENTATION OF RESULTS

In this section, the results achieved by numerically solving the coupled system of self-similar equations (14) to (18) and (23) will be presented.

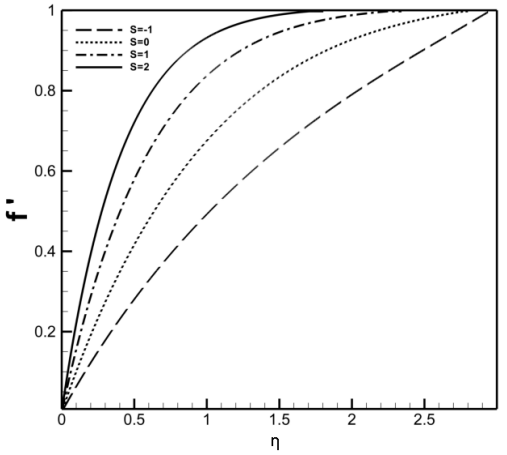

(a)

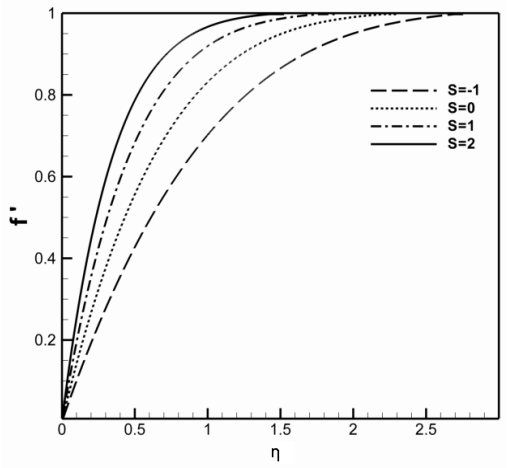

(b)

Fig. 2. Distributions of f' profiles for different values of S parameter when (a) $\lambda = 0.1$ and (b) $\lambda = 0.9$.

As we know, S parameter represents the suction into the plate $(S > 0)$ or blowing out of it $(S < 0)$. Here, the effects of transpiration rate S on dimensionless velocity profiles in x and y directions are presented for three dimensional cases, defined with $\lambda = 0.1$ and $\lambda = 0.9$, in Figs. 2 and 3. According to these two figures, the thickness of the viscous layer in the region close to the plate is higher for negative values of S compared to that when $S > 0$. Moreover, it is clear from (a) and (b) parts of these figures that as the stagnation flow patterns approach the axisymmetric case, $\lambda = 0.9$, the viscous layer thickness decreases and the amount of velocity components increases at any specified values of S and η. Furthermore, distributions of the velocity component in z-direction along with $f(\eta)$ and $g(\eta)$ functions are illustrated in figure (4) in terms of selected values of S and λ parameters. As it is shown in this figure, the more the amount of S, the more the value of $f(\eta)$ and, also, the absolute value of w-component will be in all three dimensional cases. Besides, it is revealed that the influence of suction or blowing intensity on $g(\eta)$ distributions is more considerable when $\lambda \to 0$.

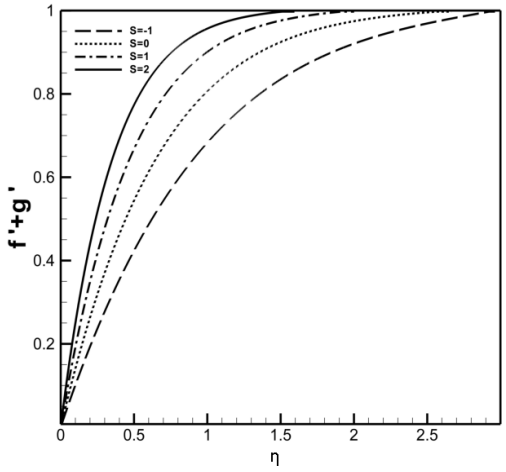

(a)

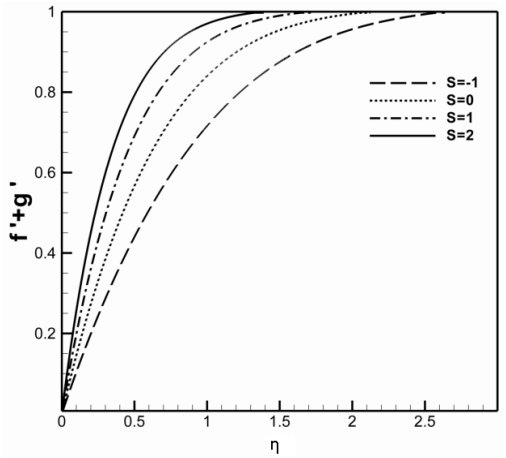

(b)

Fig. 3. Distributions of $f'+g'$ profiles for different values of S parameter when (a) $\lambda = 0.1$ and (b) $\lambda = 0.9$

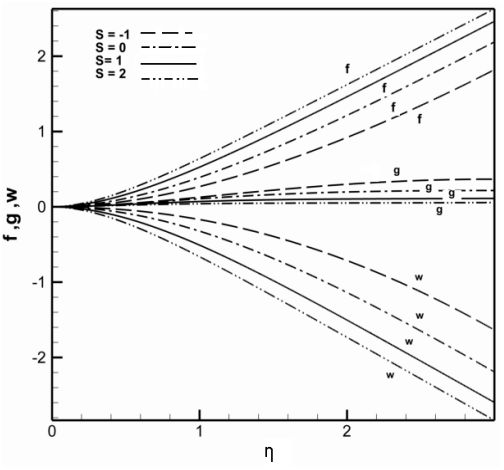

(a)

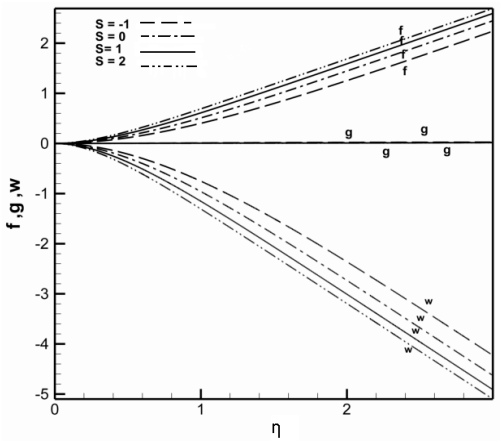

(b)

Fig. 4. Distributions of w-component of velocity, $f(\eta)$ and $g(\eta)$ functions for different values of S parameter when (a) $\lambda = 0.1$ and (b) $\lambda = 0.9$.

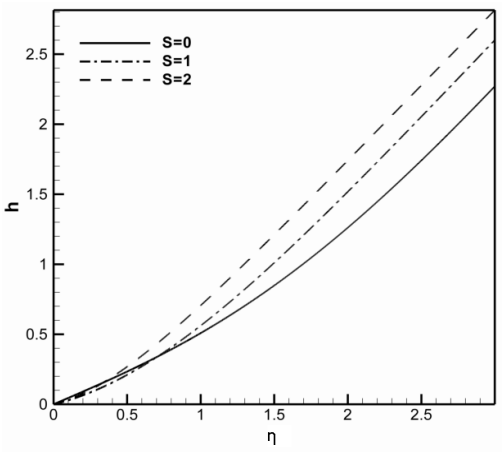

(a)

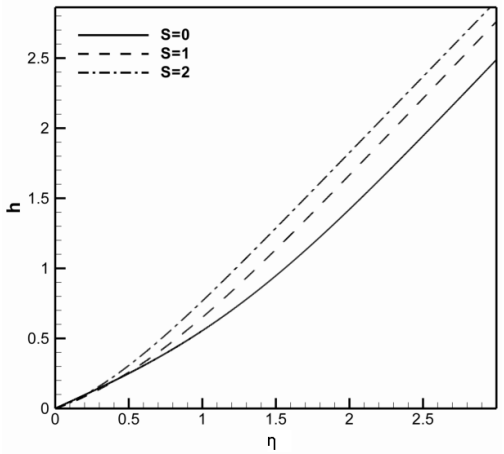

(b)

Fig. 5. Distributions of $h(\eta)$ profiles for different values of S parameter when (a) $\lambda = 0.1$ and (b) $\lambda = 0.9$.

In figure (5), the variations of $h(\eta)$ function with respect to η for different values of S and λ parameters are illustrated. It can be found out from this figure that with enhancement of suction intensity, the value of $h(\eta)$ function increases as well.

The pressure profiles inside the boundary layer are depicted in Fig. 6 for different values of transpiration rate S and velocity ratio λ. As it is captured, the increase in the value of S parameter from -1 to 2 causes the pressure gradients to increase in the region close to the plate. This phenomenon brings about the increase in the absolute value of pressure at any specified values of η. Also comparing the results in parts (a) and (b) of this figure reveals the important note that the pressure gradients in the vicinity of the plate are more considerable for higher value of λ, $\lambda = 0.9$ for instance.

Dimensionless temperature distributions versus η in terms of different values of S parameter and selected values of Pr number are depicted in Fig. 7 for $\lambda = 0.1$ and in Fig. 8 for $\lambda = 0.9$. As it can be found out from these two figures, the increase of S parameter from -1.0 to 2.0 brings about the decrease in the thermal boundary layer thickness and increase in the temperature gradient in the region near the wall at any fixed values of λ and Pr numbers. It is worth noting that when the fluid is blown out of the plate, the temperature gradient near the plate tends to zero especially for fluids with a high Pr number. It means that there is no considerable heat transfer between the plate and fluid in such a situation. The obtained results also revealed that the increase of Pr number results in decrease in the thermal boundary layer thickness at any value of λ, as expected.

As it was mentioned before, γ is a parameter being the ratio of the strength of outer shear flow to the outer normally impinging flow. In Figs. 9 to 12, sample forms of streamlines are presented for different values of γ parameter when $S = 0.0$, λ=0.5 . These streamlines are obtained by using the computed velocity components and are

illustrated in the $x-\eta$ plane when $y=0$. Fig. 9 shows the obtained streamlines for the case of $\gamma=0$. As it can be noticed in Figs. 10 and 11, the flow pattern is inclined to the left-hand side for positive values of γ. The more the γ parameter, the more deviation with respect to normal direction on the plate is captured for streamlines. Another considerable point in these two figures is that with increase of γ parameter, the distance between the stagnation point position and the origin of the coordinate system enhances. Moreover, Fig. 12 reveals that for negative value of γ, the streamlines are deviated to the right-hand side.

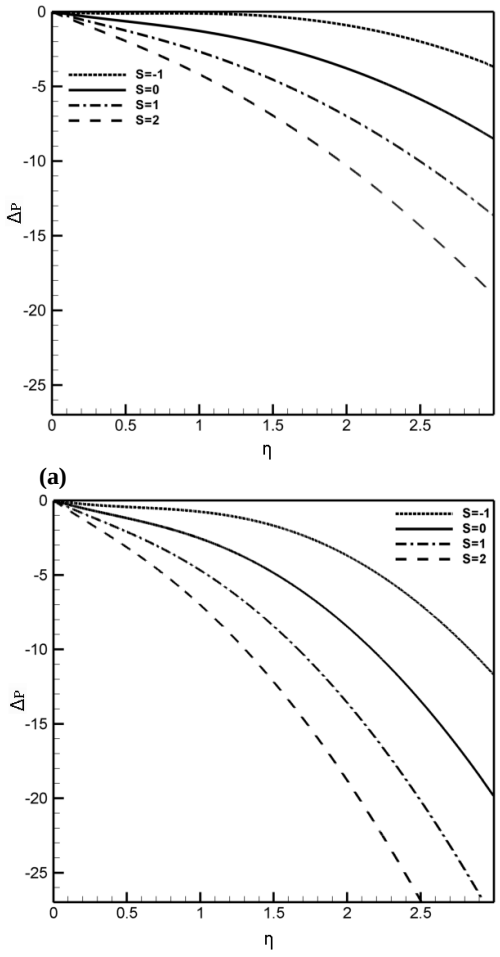

Fig. 6. Distributions of pressure profiles for different values of S parameter when (a) $\lambda=0.1$ and (b) $\lambda=0.9$.

Next, the distributions of shear stress components in x and y directions are shown in Figs. 13 and 14 for $\gamma=0.0$ and $\gamma=1.0$, respectively, and in terms of different values of transpiration rate S and velocity ratio λ. According to these two figures, the shear stress component in y-direction is independent of γ and λ parameters; however, the increase of the value of S number causes this component to enhance. Besides, as it is captured in Figs. 13 and 14, the x-component of the shear stress increases as the flow pattern crosses the line from two-dimensionality towards the axisymmetric three-dimensionality. Another important note is that the more the value of γ, the more the amount of shear stress component in x-direction will be at any value of λ.

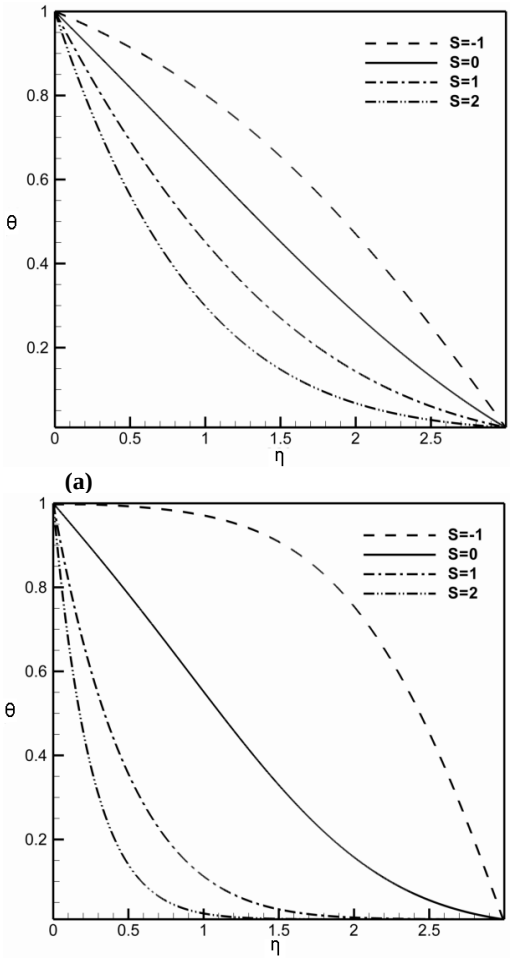

Fig. 7. Distributions of dimensionless temperature profiles for $\lambda=0.1$ and different values of S parameter when (a) $\Pr=0.5$ and (b) $\Pr=2.0$.

In the next three figures, the influences of transpiration rate S along with γ and λ numbers on the position of the stagnation point are investigated. As it is clear in these figures, the increase of γ parameter causes the stagnation point to be shifted away from the origin of the coordinate system at any fixed value of transpiration rate S and velocity ratio λ. Moreover, it is revealed that in an obliquely impinging flow, the stagnation point is less displaced when the fluid is sucked into the plate $(S>0)$ in comparison with the situation where the fluid is blown out of the plate $(S<0)$. Another interesting point is that as the flow patterns move toward the axisymmetric case $(\lambda\to 1.0)$, the

stagnation point becomes closer to the origin at any amount of transpiration rate. This phenomenon is more noticeable in high values of γ parameter.

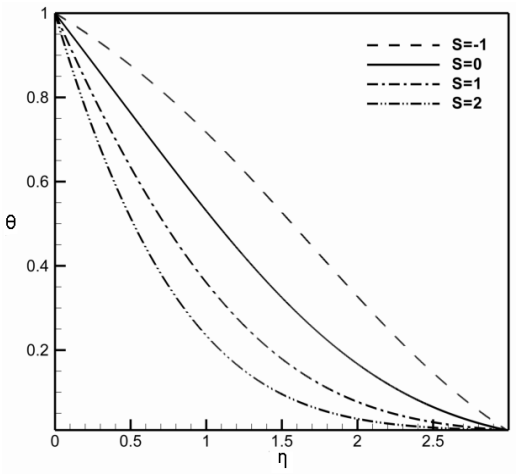

(a)

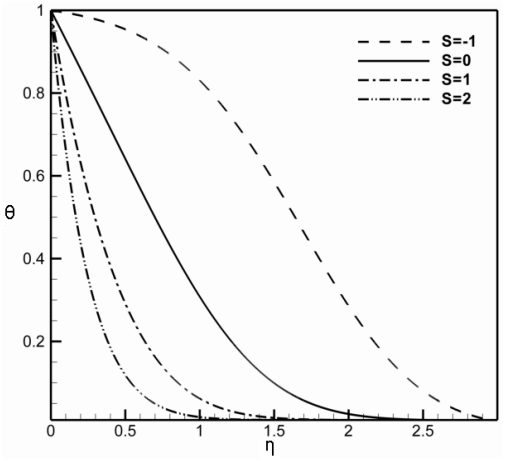

(b)

Fig. 8. Distributions of dimensionless temperature profiles for $\lambda = 0.9$ and different values of S parameter when (a) $\Pr = 0.5$ and (b) $\Pr = 2.0$.

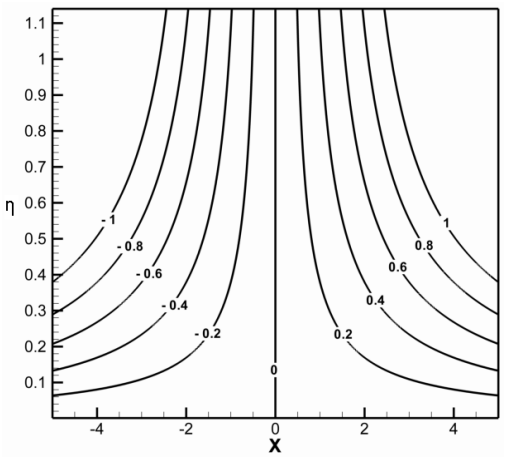

Fig. 9. Streamlines in $x-\eta$ plane for the case of $\gamma = 0.0$ when $\lambda = 0.5$, S=0.0.

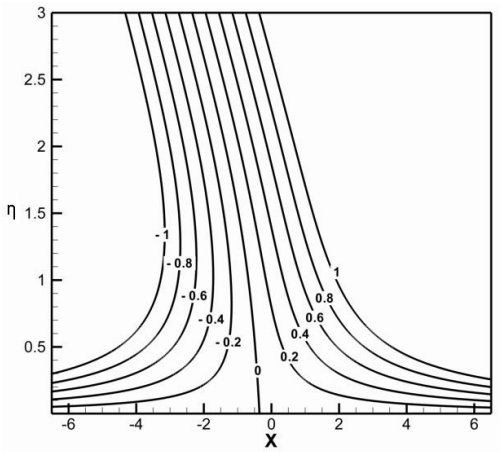

Fig. 10. Streamlines in $x-\eta$ plane for the case of $\gamma = 1.0$ when $\lambda = 0.5$, S=0.0.

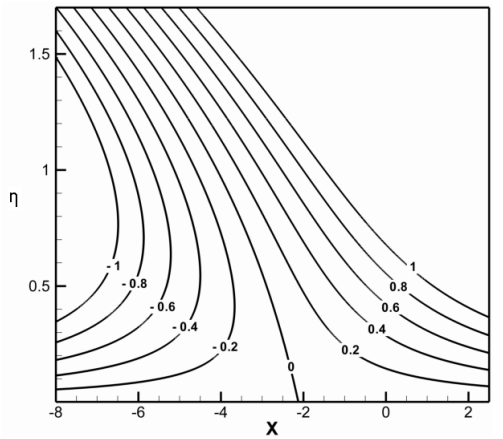

Fig. 11. Streamlines in $x-\eta$ plane for the case of $\gamma = 3.0$ when $\lambda = 0.5$, S=0.0.

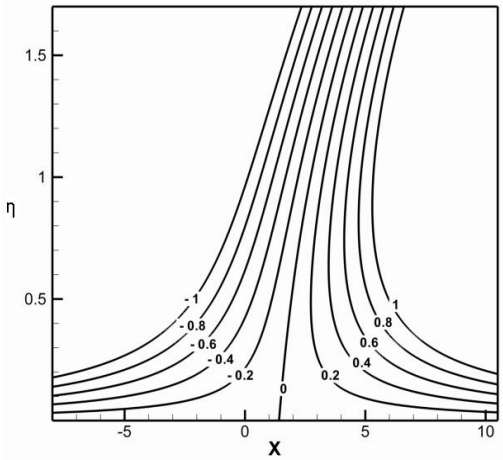

Fig. 12. Streamlines in $x-\eta$ plane for the case of $\gamma = -2.0$ when $\lambda = 0.5$, S=0.0.

With the enhancement of Pr number, the temperature gradient increases in the region close to the wall. This fact is intended to be shown in Fig. 18 for selected values of λ parameters when $S = 0.1$. This figure illustrates that there is a considerably more heat transfer between the plate and fluids with high Pr number compared to the fluids with low Pr

number. Moreover, as it is captured, increase of the velocity ratio λ results in increase of the dimensionless temperature gradient at $\eta = 0.0$.

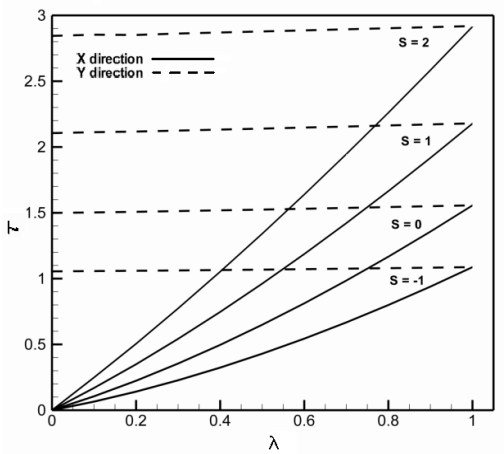

Fig. 13. Distributions of shear stress components in x and y directions in terms of different values of λ and S parameters when $\gamma = 0.0$.

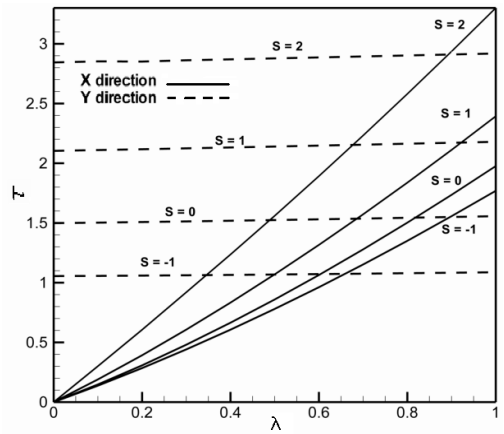

Fig. 14. Distributions of shear stress components in x and y directions in terms of different values of λ and S parameters when $\gamma = 1.0$.

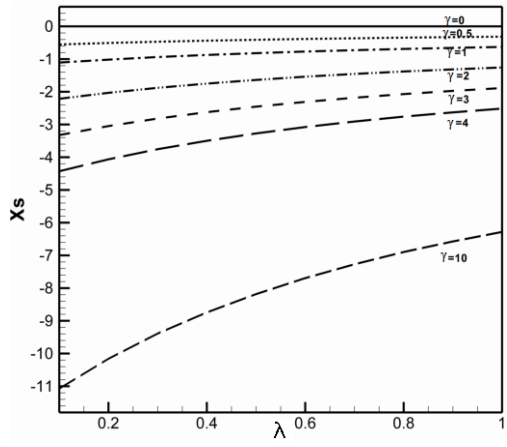

Fig. 15. Stagnation point position for different values of λ and γ parameters when $S = -1.0$.

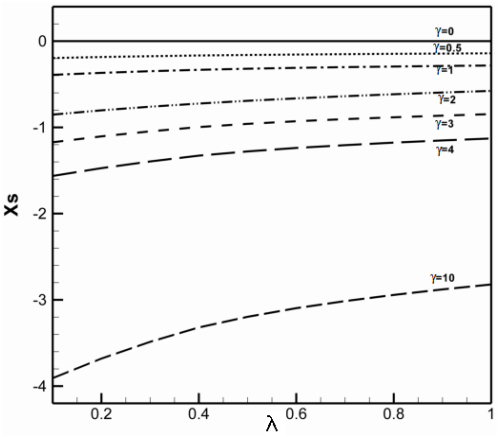

Fig. 16. Stagnation point position for different values of λ and γ parameters when $S = 0.0$.

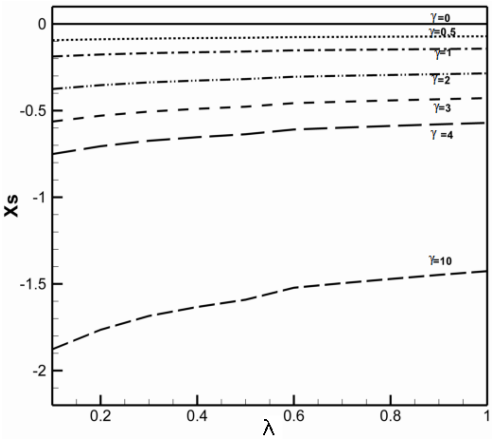

Fig. 17. Stagnation point position for different values of λ and γ parameters when $S = 2.0$.

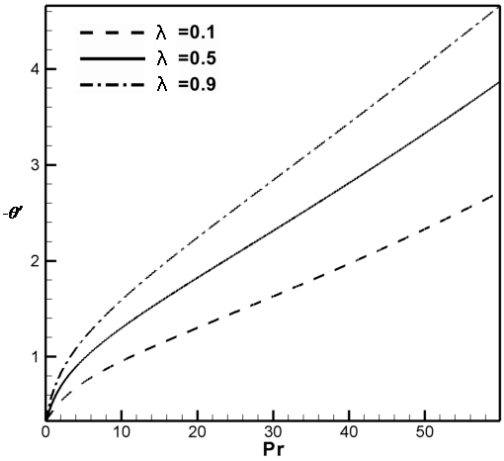

Fig. 18. Dimensionless temperature gradient distributions at $\eta = 0.0$ versus Pr number in terms of selected values of λ parameter when $S = 0.1$

5. CONCLUSION

In this paper, the unsteady three dimensional stagnation-point flow and heat transfer of a viscous, incompressible fluid yet obliquely impinging on a

flat plate with transpiration was investigated. By using firstly introduced similarity transformations, an exact solution of the governing Navier-Stokes and energy equations was obtained when an unsteady external flow with strain rate $a/(1-at)$ impinges obliquely on the flat plate. This flow consists of stagnation-point flow (Hiemenz) and a tangential component. The relative importance of these two flows is measured by a parameter γ. The obtained results were presented for a wide range of parameters characterizing the problem. The results revealed that the transpiration rate S has a great influence on distributions of velocity components, temperature and pressure. Moreover, it was shown that γ and λ parameters have no effect on the amount of y-component shear stress, however, increase of the value of these two parameters causes the value of shear stress component in x-direction to enhance. It was also shown that the main consequence of the free stream obliqueness is to shift the location of the stagnation point towards the incoming flow.

6. REFERENCES

Davey, A. (1951). Boundary Layer Flow at a Saddle Point of Attachment. *Journal of Fluid Mechanics* 63, 593-610.

Shokrgozar, A. and A. B. Rahimi (2009). Three-Dimensional Stagnation Flow and Heat Transfer on a Flat Plate with Transpiration. *Journal of Thermophysics and Heat transfer* 23, 513-521.

Rahimi, A. B. and M. Esmaeilpour (2010). Axisymmetric Stagnation Flow Obliquely Impinging on a Moving Circular Cylinder with Uniform Transpiration. *International Journal for Numerical Methods in Fluid* 65, 1084-1095.

Rahimi, A. B. and R. Saleh (2007). Axisymmetric Stagnation-Point Flow and Heat Transfer of a Viscous Fluid on a Rotating Cylinder with Time-Dependent Angular Velocity and Uniform Transpiration. *Journal of Fluid Engineering* 129, 106-115.

Rahimi, A. B. and R. Saleh (2008). Similarity Solution of Unaxisymmetric Heat Transfer in Stagnation-Point Flow on a Cylinder with Simultaneous Axial and Rotational Movements. *Journal of Heat Transfer* 130(5), 054502.1-054502.5.

Rahimi, A. B. and V. Mossavinik (2007). Axisymmetric Stagnation-Point Flow and Heat Transfer Obliquely Impinging on a Rotating Circular Cylinder. *International Journal of Engineering* 20, 67-82.

Devi, D. S., H. S. Takhar and G. Nath (1986). Unsteady Three Dimensional Boundary Layer Flow due to Stretching Surface. *International Journal of Heat and Mass Transfer* 29, 1996-1999.

Cheng, E. H., M. N. Ozisik and J. C. Williams (1971). Nonsteady Three-Dimensional Stagnation-Point Flow. *Journal of Applied Mechanic* 38, 282-287.

Laboropulu, F., J. M. Dorrepaal and O. P. Chandna (1996). Oblique Flow Impinging on a Wall with Suction and Blowing. *Acta Mech*, 163, 15-25.

Homman, F. Z. (1936). Der EINFLUSS GROSSER Zanhighkeit bei der strmung um den Zylinder und um die Kungel. *Zeitschrift fuer angewandte Mathematik und Mechanik* 16(3), 153–164.

Niimi, H., M. Minamiyama and S. Hanai (1981). Steady Axisymmetrical Stagnation-Point Flow Impinging obliquely on a wall. *Journal of The physical Society of Japan* 50, 7-8.

Dorrepaal, J. M. (1986). An Exact Solution of The Navier-Stokes Equation Which Describes Non-Orthogonal Stagnation Point Flow in Two Dimensions. *Journal of Fluid Mechanic* 163, 141-147.

Stuart, J. T. (1959). The Viscous Flow near a Stagnation Point when the External Flow has Uniform Vorticity. *Journal of Aerospace Science* 26, 124-125.

Hiemenz, K. (1911). Boundary Layer for a Homogeneous Flow around a Dropping Cylinder. *Dinglers Polytechnuc Journal* 326, 321-324.

Tamada, K. (1979). Two-Dimensional Stagnation Point Flow Impinging Obliquely on a plane wall. *Journal of The physical Society of Japan* 46(1), 310-311.

Howarth, L. (1954). The Boundary Layer in Three-Dimensional Flow, Part II: The Flow near Stagnation Point. *Philosophical Magazine* 42, 1433–1440.

Reza, M. and A. S. Gupta (2005). Steady Two-Dimensional Oblique Stagnation-Point Flow towards a Stretching surface. *Journal of Fluid Dynamics Research* 37, 334-340.

Bachok, N., A. Ishak and I. Pop (2010). Unsteady Three-Dimensional Boundary Layer Flow due to Shirinking sheet. *Applied Mathematics and Mechanics* 31, 1421-1428.

Weidman, P. D. and V. Putkaradze (1976). Axisymmetric Stagnation Flow Obliquely Impinging on a Circular Cylinder. *European Journal of Engineering* 32, 541-553.

Saleh, R. and A. B. Rahimi (2004). Axisymmetric Stagnation-Point Flow and Heat Transfer of a Viscous Fluid on a Moving Cylinder with Time-Dependent Axial Velocity and Uniform Transpiration. *Journal of Fluid Engineering* 12, 997-1005.

Gorla, R. S. R. (1976). Heat Transfer in an Axisymmetric Stagnation Flow on a Cylinder, *Applied Science Research* 32, 541-553.

Gorla, R. S. R. (1977). Unsteady Laminar Axisymmetric Stagnation Flow over a Circular Cylinder. *Developments in Mechanics* 9, 286-288.

Gorla, R. S. R. (1978). Nonsimilar Axisymmetric Stagnation Flow on a moving Cylinder. *International Journal of Engineering Science* 16, 392-400.

Gorla, R. S. R. (1978). Transient response behavior of an Axisymmetric Stagnation Flow on a Circular Cylinder Due to time-dependent free stream velocity. *Letters in Applied Engineering Science* 16, 493-502.

Gorla, R. S. R. (1979). Unsteady Viscous Flow in the Vicinity of an Axisymmetric Stagnation-Point on a Cylinder. *International Journal of Engineering Science* 17, 87-93.

Chiam, T. M. (1994). Stagnation Point Flow towards a Stretching Plate. *Journal of The physical Society of Japan* 63(6), 2441-2444.

Mahapatra, T. R. and A. S. Gupta (2002). Heat Transfer in Stagnation-Point Flow towards a Stretching sheet. *Heat and mass Transfer* 38, 517-521.

Wang, V. (1984). The Three Dimensional Flow Due to a Stretching Flat Surface. *Physics of Fluids* 27, 1915-1917.

Lok, Y. Y. and N. Amin (2006). Non-Orthogonal Stagnation Point Flow towards a Stretching Sheet. *International Journal of Non-Linear Mechanics* 41, 622-627.